



Improvement of electrochemical properties of $\text{Li}_{1.1}\text{Al}_{0.05}\text{Mn}_{1.85}\text{O}_4$ achieved by an AlF_3 coating

Dong-Ju Lee^{a,c}, Ki-Soo Lee^{a,c}, Seung-Taek Myung^{b,*}, Hitoshi Yashiro^b, Yang-Kook Sun^{a,c,**}

^a Department of WCU Energy Engineering, Hanyang University, Seoul 133-791, South Korea

^b Department of Chemical Engineering, Iwate University, 4-3-5 Ueda, Morioka, Iwate 020-8551, Japan

^c Department of Chemical Engineering, Hanyang University, Seoul 133-791, South Korea

ARTICLE INFO

Article history:

Received 17 August 2010

Accepted 16 September 2010

Keywords:

AlF_3
Coating
Spinel
Cathode
Lithium
Battery

ABSTRACT

The electrochemical performance of AlF_3 -coated $\text{Li}_{1.1}\text{Al}_{0.05}\text{Mn}_{1.85}\text{O}_4$ spinel was investigated. The morphology of the AlF_3 -coated $\text{Li}_{1.1}\text{Al}_{0.05}\text{Mn}_{1.85}\text{O}_4$ was observed by SEM and TEM, and the thickness of the coating layer was approximately 10 nm. Capacity retention and rate capability were substantially improved by the AlF_3 -coating, as compared to pristine $\text{Li}_{1.1}\text{Al}_{0.05}\text{Mn}_{1.85}\text{O}_4$. Manganese dissolution was also dramatically reduced for the AlF_3 -coated $\text{Li}_{1.1}\text{Al}_{0.05}\text{Mn}_{1.85}\text{O}_4$, which may reflect lower impedance for the coated spinel. The thermal stability of the AlF_3 -coated $\text{Li}_{1.1}\text{Al}_{0.05}\text{Mn}_{1.85}\text{O}_4$ was improved, exhibiting an exothermic reaction at higher temperature with reduced heat generation, compared to the pristine $\text{Li}_{1.1}\text{Al}_{0.05}\text{Mn}_{1.85}\text{O}_4$.

© 2010 Elsevier B.V. All rights reserved.

1. Introduction

Many automobile manufacturers have invested in electric vehicles (EV) and hybrid electric vehicles (HEV) over the last 10 years. Li-ion batteries have been considered as power sources for these transportation systems, due to their high working voltage, high energy density and long cycle life. Spinel type LiMn_2O_4 is a promising material as cathode materials for Li-ion batteries due to good safety, low cost, abundance, nontoxicity, and high-rate capability [1–3]. However, poor cycle stability during repeated cycling occurs at room temperature and is more severe at high temperature. Mn^{3+} ions cause the Jahn–Teller distortion which leads to capacity fading at room temperature [4,5]. In addition, the spinel LiMn_2O_4 electrode degrades by Mn dissolution from disproportionate reactions of Mn^{3+} ($2\text{Mn}^{3+} \rightarrow \text{Mn}^{2+} + \text{Mn}^{4+}$) in the presence of acidic species in an electrolyte. Various strategies have been employed to overcome these issues. For example, the poor cycle stability of spinel LiMn_2O_4 has been improved by cation substitution (Li, Al, Fe, Ni, Co, and Cr) at the Mn site [6–12]. Moreover, diverse coatings on the

surface of the cathode materials have been adopted to enhance the cycling stability of the spinel LiMn_2O_4 cathode. MgO , Al_2O_3 , ZnO , BiOF , ZrO_2 , and SiO_2 coatings showed acceptable improvement in the cycling stability [13–18].

Recently, we reported the improvement of the electrochemical performance of layered cathode materials with an AlF_3 coating [19–26]. For these prior investigations, we suggested that the AlF_3 coating layer played an important role in protecting the layered cathode material from HF attack in the electrolyte, thereby improving the capacity, retention, rate capability, and thermal stability of the cathode materials [19–26]. However, AlF_3 coating has not been attempted on a spinel cathode material. In this work, an AlF_3 coating was applied to spinel $\text{Li}_{1.1}\text{Al}_{0.05}\text{Mn}_{1.85}\text{O}_4$, and the resulting electrochemical performance and thermal stability were investigated.

2. Experimental

To synthesize $\text{Li}_{1.1}\text{Al}_{0.05}\text{Mn}_{1.85}\text{O}_4$, Mn_3O_4 as a starting material was synthesized via a co-precipitation method previously described [27]. The prepared Mn_3O_4 was mixed with stoichiometric amounts of LiOH and $\text{Al}(\text{OH})_3$. The mixture was calcined at 850°C for 15 h in an air atmosphere. The as-synthesized powder was immersed in a mixture of an aluminum nitrate nonahydrate aqueous solution and an ammonium fluoride aqueous solution to produce the AlF_3 -coated spinel compound. The solution containing

* Corresponding author. Tel.: +81 19 621 6345; fax: +81 19 621 6345.

** Corresponding author at: Department of Chemical Engineering, Hanyang University, Seoul 133-791, South Korea. Tel.: +82 2 2220 0524; fax: +82 2 2282 7329.

E-mail addresses: smyung@iwate-u.ac.jp (S.-T. Myung), yksun@hanyang.ac.kr (Y.-K. Sun).

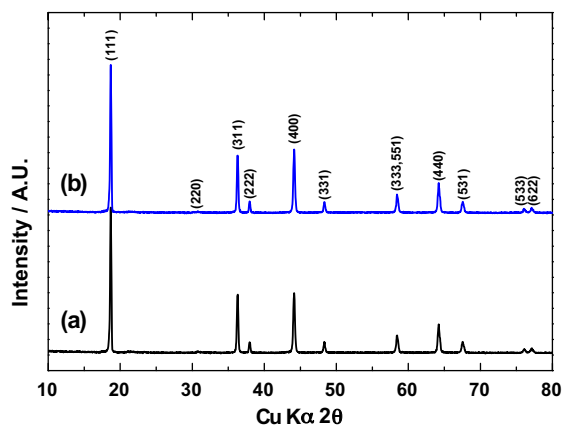


Fig. 1. Powder XRD patterns of (a) as-synthesized $\text{Li}_{1.1}\text{Al}_{0.05}\text{Mn}_{1.85}\text{O}_4$ and (b) AlF_3 -coated $\text{Li}_{1.1}\text{Al}_{0.05}\text{Mn}_{1.85}\text{O}_4$.

the cathode powder was constantly stirred for 5 h at 80°C and then filtered. The obtained powder was heated at 400°C for 5 h under a N_2 gas to avoid the formation of Al_2O_3 .

The crystal structure and purity of the products were analyzed by X-ray diffraction (XRD, Rint-2000, Rigaku) using $\text{Cu K}\alpha$ radiation. The morphology of the prepared powders was observed by transmission electron microscopy (TEM, JEM 2010, JEOL). The chemical compositions of the resulting powders were determined by atomic absorption spectroscopy (AAS) (Vario 6, Analyticjena, Germany).

Cathodes were fabricated by blending the prepared powders, Super P carbon black, and polyvinylidene fluoride (85:7.5:7.5) in *N*-methyl-2-pyrrolidone. The slurry was coated onto Al foil and roll-pressed at 120°C in air. The electrodes were vacuum dried overnight at 120°C prior to use. Cell tests were performed using a R2032 coin-type cell adopting Li metal as the anode. The electrolyte solution was 1 mol dm^{-3} LiPF_6 in an ethylene carbonate–dimethyl carbonate (1:2 in volume, PANAX ETEC, Co., Ltd.). The cathode and anodes were separated by a porous polypropylene film. All cells were prepared in an Ar-filled dry box. The assembled cells were charged and discharged within a voltage range of 3.0–4.3 V with a constant current density of 50 mA g^{-1} (0.5 C-rate) at 55°C . Cycle-life tests were performed at the same voltage and temperature conditions.

For HF titration, cells cycled at 55°C (adapting the Li metal as the anode) were carefully disassembled, and the resulting contents were washed thoroughly with Li salt-free solvent for 1 week in a glove box. An aqueous solution of NaOH (Kanto) with Bromothymol Blue (BTB, Aldrich) as an indicator was used for the titration of the used electrolyte. To confirm the presence of by-products on the surface of the active materials after extensive cycling, the active cycled materials were examined by time-of-flight secondary ion mass spectroscopy (ToF-SIMS, ULVAC-PHI TFS2000, Perkin Elmer) at 10^{-9} Torr. This instrument was also equipped with a liquid Ga ion source and pulse electron flooding. During the analysis, the targets were bombarded by pulsed 15 keV Ga^+ beams. The total collection time was 300 s over a $12\text{ }\mu\text{m} \times 12\text{ }\mu\text{m}$ area. AC-impedance measurements were performed using a Zahner Elektrik IM6 impedance analyzer over a frequency range from 1 MHz to 1 mHz, with an amplitude of 10 mV. Half-cells were charged to 4.3 V, and the charged electrodes were stored in fresh electrolyte at 55°C . The aged electrolytes were then examined to measure dissolved Mn by AAS. Differential scanning calorimetry (DSC) was performed for the positive electrode materials by fully charging the coin cell to 4.3 V at a constant current and constant voltage. The measurements were performed in a differential scanning calorimeter (DSC, 200 PC, Netzsch) using a temperature scan rate of 1°C min^{-1} .

3. Results and discussion

XRD patterns of the as-synthesized and AlF_3 treated powders are shown in Fig. 1. Both products were confirmed as cubic spinel structures with the $Fd3m$ space group. The AlF_3 -coated spinel material exhibited no indication of Al-related impurity phases. The chemical composition of the as-synthesized was verified as $\text{Li}_{1.1}\text{Al}_{0.05}\text{Mn}_{1.85}\text{O}_4$. Lattice parameters were calculated by a least squares method from the diffraction patterns. Calculated lattice parameters for the pristine and AlF_3 -coated $\text{Li}_{1.1}\text{Al}_{0.05}\text{Mn}_{1.85}\text{O}_4$ were $8.198(1)\text{ \AA}$ and $8.198(2)\text{ \AA}$, respectively, indicating that Al or F were incorporated into the parent $\text{Li}_{1.1}\text{Al}_{0.05}\text{Mn}_{1.85}\text{O}_4$ by the AlF_3 coating.

TEM images of the pristine and AlF_3 -coated $\text{Li}_{1.1}\text{Al}_{0.05}\text{Mn}_{1.85}\text{O}_4$ are shown in Fig. 2. The pristine material shows smooth edge lines and no foreign material, as shown in Fig. 2a. However, a thin coating layer was clearly observed for the coated spinel in

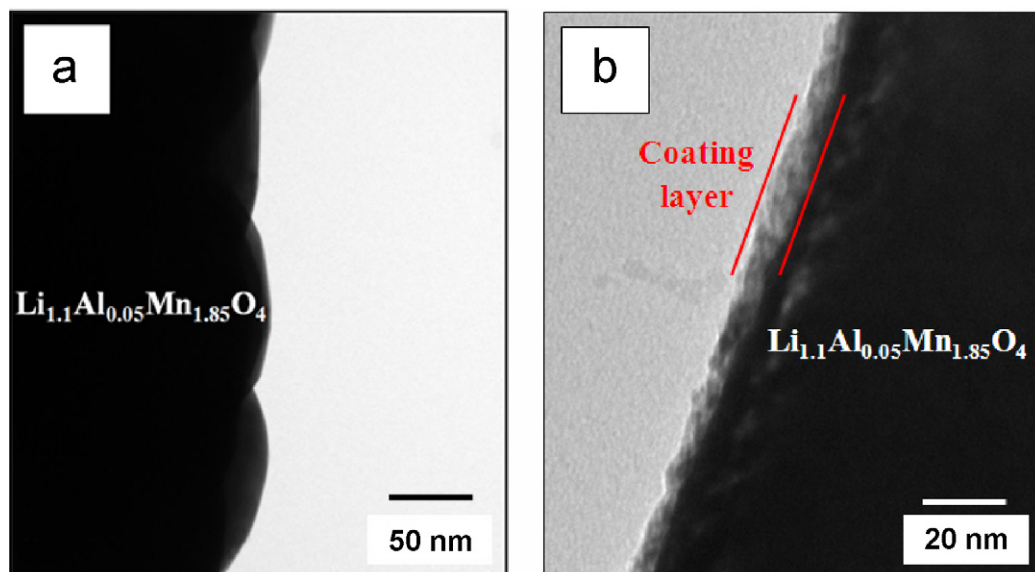


Fig. 2. Bright-field TEM images of (a) pristine $\text{Li}_{1.1}\text{Al}_{0.05}\text{Mn}_{1.85}\text{O}_4$ and (b) AlF_3 -coated $\text{Li}_{1.1}\text{Al}_{0.05}\text{Mn}_{1.85}\text{O}_4$.

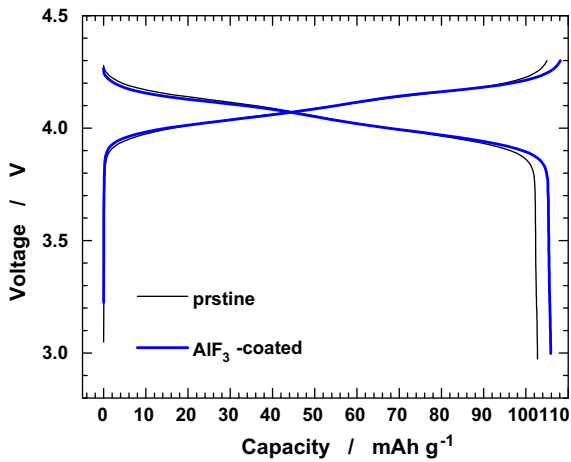


Fig. 3. Comparison of the first charge and discharge curves of (a) Li/pristine $\text{Li}_{1.1}\text{Al}_{0.05}\text{Mn}_{1.85}\text{O}_4$ and Li/AlF₃-coated $\text{Li}_{1.1}\text{Al}_{0.05}\text{Mn}_{1.85}\text{O}_4$ cells at 55 °C.

Fig. 2b, of which the thickness was approximately 10–15 nm. As confirmed by the XRD data of Fig. 1b, the TEM results indicate that the $\text{Li}_{1.1}\text{Al}_{0.05}\text{Mn}_{1.85}\text{O}_4$ was coated by the AlF₃ nanolayer, and the layer resides only on the surface of the spinel compound. The low heat treatment temperature for the AlF₃ coating did not likely allow for the formation of a solid solution between AlF₃ and $\text{Li}_{1.1}\text{Al}_{0.05}\text{Mn}_{1.85}\text{O}_4$. Otherwise, the resulting lattice parameter should vary after the heat treatment.

Electrochemical properties of the pristine and AlF₃-coated $\text{Li}_{1.1}\text{Al}_{0.05}\text{Mn}_{1.85}\text{O}_4$ were also compared to determine the effect of the AlF₃ coating in Fig. 3. Thus, charge and discharge tests were made by applying a constant current of 50 mA g^{-1} (0.5 C-rate) at 55 °C. The first charge and discharge curves show typical potential plateaus of spinel compounds at the 4 V region, originating from the $\text{Mn}^{3+}/\text{Mn}^{4+}$ redox couples. The discharge capacity for the AlF₃-coated $\text{Li}_{1.1}\text{Al}_{0.05}\text{Mn}_{1.85}\text{O}_4$ (106 mAh g^{-1}) was slightly greater than that of the pristine (102 mAh g^{-1}). The slight change in the capacity was due to the lower resistance of the cell, likely achieved by the presence of the AlF₃ coating layer on the spinel $\text{Li}_{1.1}\text{Al}_{0.05}\text{Mn}_{1.85}\text{O}_4$. Cycling data of the pristine and AlF₃-coated $\text{Li}_{1.1}\text{Al}_{0.05}\text{Mn}_{1.85}\text{O}_4$ are shown in Fig. 4. The pristine $\text{Li}_{1.1}\text{Al}_{0.05}\text{Mn}_{1.85}\text{O}_4$ retained its original capacity of approximately 85.3% at the 100th cycle. Meanwhile, the AlF₃-coated $\text{Li}_{1.1}\text{Al}_{0.05}\text{Mn}_{1.85}\text{O}_4$ had a higher capacity and improved capacity retention, displaying 96.2% retention of the initial discharge capacity at the 100th cycle. The capacity reten-

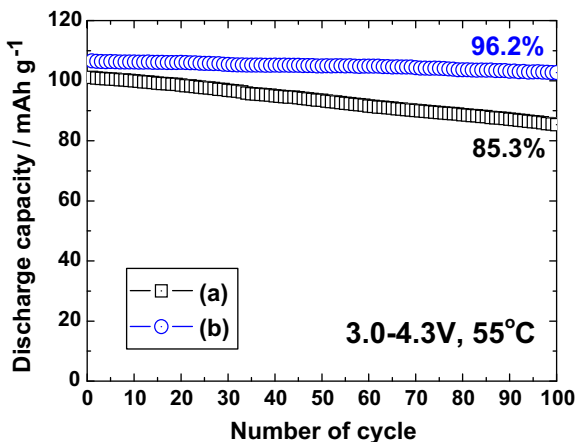


Fig. 4. Cycling performance of (a) pristine $\text{Li}_{1.1}\text{Al}_{0.05}\text{Mn}_{1.85}\text{O}_4$ and (b) AlF₃-coated $\text{Li}_{1.1}\text{Al}_{0.05}\text{Mn}_{1.85}\text{O}_4$ cells during 100 cycles at a current density of 50 mA g^{-1} (0.5 C) at 55 °C.

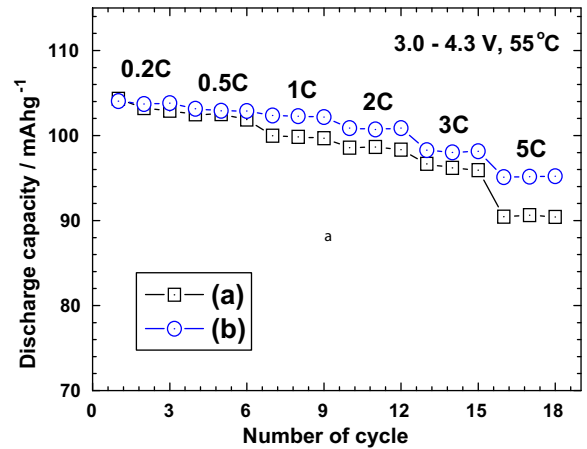


Fig. 5. Rate capability of (a) pristine $\text{Li}_{1.1}\text{Al}_{0.05}\text{Mn}_{1.85}\text{O}_4$ and (b) AlF₃-coated $\text{Li}_{1.1}\text{Al}_{0.05}\text{Mn}_{1.85}\text{O}_4$ at 55 °C.

tion was similar to the BiOF-coated $\text{Li}_{1.1}\text{Al}_{0.05}\text{Mn}_{1.85}\text{O}_4$ [18], which showed 96.1% capacity retention under the same conditions. As a result, the AlF₃ coating on the spinel compound was comparable to the BiOF coating with respect to the cycling performance.

Fig. 5 presents the discharge capacity of the pristine and AlF₃-coated $\text{Li}_{1.1}\text{Al}_{0.05}\text{Mn}_{1.85}\text{O}_4$ cells at various currents in a range of 3.0–4.3 V at 55 °C. AlF₃-coated $\text{Li}_{1.1}\text{Al}_{0.05}\text{Mn}_{1.85}\text{O}_4$ exhibited greater discharge capacity than the pristine $\text{Li}_{1.1}\text{Al}_{0.05}\text{Mn}_{1.85}\text{O}_4$ at all currents. Based on these electrochemical measurements, the AlF₃-coating on the surface of $\text{Li}_{1.1}\text{Al}_{0.05}\text{Mn}_{1.85}\text{O}_4$ spinel was substantially more effective in enhancing capacity, retention, and rate capability.

As shown in Fig. 4, the most likely reason for the capacity fading was manganese dissolution from the active materials during extensive cycling. To estimate the amount of Mn dissolution, both cells were charged to 4.3 V, and the charged electrodes were transferred to fresh electrolyte. The electrolytes were stored for 4 weeks at 55 °C and examined by AAS. As shown in Fig. 6, less Mn was dissolved for the AlF₃-coated $\text{Li}_{1.1}\text{Al}_{0.05}\text{Mn}_{1.85}\text{O}_4$. Specifically, the dissolved amount of Mn for the pristine material was approximately 63 ppm during the first week, while, the AlF₃-coated $\text{Li}_{1.1}\text{Al}_{0.05}\text{Mn}_{1.85}\text{O}_4$ showed less Mn dissolution in the electrolyte, with a concentration of approximately 27 ppm. After 4 weeks, the Mn concentrations for the pristine and coated cells were 280 and 80 ppm, respectively. As a result, the loss of active materials was greatly suppressed by the AlF₃ coating.

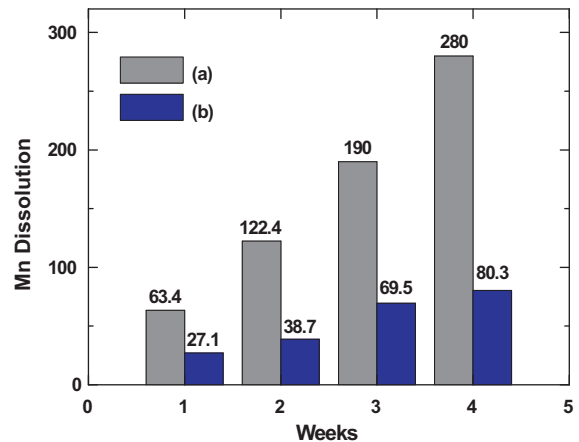


Fig. 6. Mn dissolution for the electrolyte of the fully charged (to 4.3 V) (a) Li/pristine $\text{Li}_{1.1}\text{Al}_{0.05}\text{Mn}_{1.85}\text{O}_4$ and (b) Li/AlF₃-coated $\text{Li}_{1.1}\text{Al}_{0.05}\text{Mn}_{1.85}\text{O}_4$ cells during 4 weeks at 55 °C.

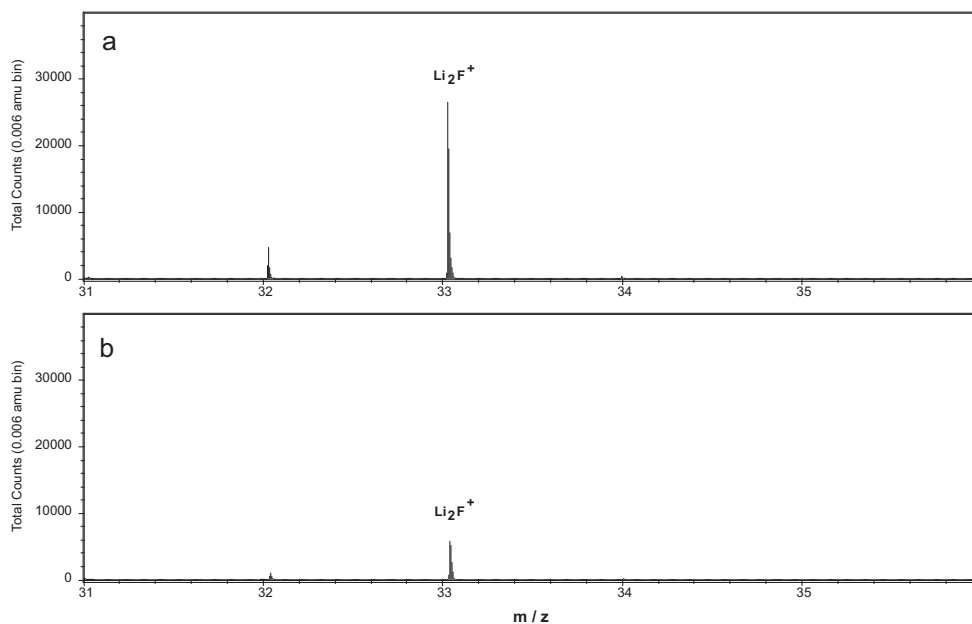


Fig. 7. ToF-SIMS results of extensively cycled electrodes at 55 °C: (a) Li_2F^+ fragments for the pristine $\text{Li}_{1.1}\text{Al}_{0.05}\text{Mn}_{1.85}\text{O}_4$ and (b) AlF_3 -coated $\text{Li}_{1.1}\text{Al}_{0.05}\text{Mn}_{1.85}\text{O}_4$.

The dissolution of the active material was significantly related to the HF contained in the electrolyte. All electrolytes have a small amount of water, less than 50 ppm, even for a lithium battery grade. The presence of water causes decomposition of the electrolyte salt, LiPF_6 , and the reaction is facilitated at elevated temperatures. At this stage, HF is significantly propagated by reaction with the water impurity. The generated HF, which is a highly reactive acid, attacks the active materials and Mn dissolution occurs, as shown in Fig. 6. Whenever LiPF_6 is decomposed, the process produces the precipitation of a LiF byproduct, which is electronically insulating, on the surface of electrode.

The cycled electrodes were observed by ToF-SIMS to determine the presence of LiF (Fig. 7). To remove the air-contaminated layer, the electrodes top surfaces were etched by Ga^+ beam for 3 s, which corresponds to 0.8 Å from the outermost surface. LiF^+ fragments appeared on both pristine and AlF_3 -coated $\text{Li}_{1.1}\text{Al}_{0.05}\text{Mn}_{1.85}\text{O}_4$, although the observed counts were quite different. The LiPF_6 salt decomposed, resulting in LiF deposition on the surface of the electrodes. More LiF was deposited on the surface of the pristine $\text{Li}_{1.1}\text{Al}_{0.05}\text{Mn}_{1.85}\text{O}_4$ because the total count for the pris-

tine material was much greater than that of the AlF_3 -coated $\text{Li}_{1.1}\text{Al}_{0.05}\text{Mn}_{1.85}\text{O}_4$. HF titration results indicated that a higher level of HF was contained in the extensively cycled electrode. Specifically, the generated HF was approximately 350 ppm for the cycled pristine $\text{Li}_{1.1}\text{Al}_{0.05}\text{Mn}_{1.85}\text{O}_4$, whereas the content for the AlF_3 -coated $\text{Li}_{1.1}\text{Al}_{0.05}\text{Mn}_{1.85}\text{O}_4$ was approximately 180 ppm. The AlF_3 coating layer potentially suppresses the breakdown of the electrolytic salt, LiPF_6 , such that less HF and LiF are formed during cycling at 55 °C. Because the HF level in the electrolyte was less than the AlF_3 -coated $\text{Li}_{1.1}\text{Al}_{0.05}\text{Mn}_{1.85}\text{O}_4$, manganese dissolution was consequently suppressed, as compared to the pristine material. As a result, higher capacity retention was observed in Fig. 4. Furthermore, less LiF was on the AlF_3 -coated $\text{Li}_{1.1}\text{Al}_{0.05}\text{Mn}_{1.85}\text{O}_4$ electrode surface, which results in the higher capacity at higher currents, as LiF is an electronic insulator. Therefore, the effectiveness of the AlF_3 coating layer was determined.

AC-impedance provides further supplemental information. Both pristine and AlF_3 -coated $\text{Li}_{1.1}\text{Al}_{0.05}\text{Mn}_{1.85}\text{O}_4$ were measured with cycling at the fully charged state (4.3 V), as described in Fig. 8. Expanded views in the inset depict the high-to-medium frequency

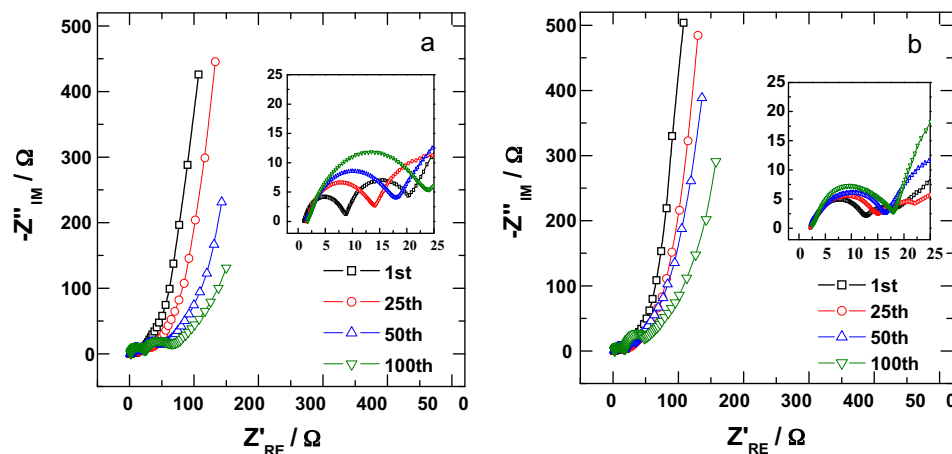


Fig. 8. Nyquist plots of (a) Li/pristine $\text{Li}_{1.1}\text{Al}_{0.05}\text{Mn}_{1.85}\text{O}_4$ and (b) Li/ AlF_3 -coated $\text{Li}_{1.1}\text{Al}_{0.05}\text{Mn}_{1.85}\text{O}_4$ cells at a charged state to 4.3 V with number of cycles; first, twenty-fifth, fiftieth, hundredth cycle.

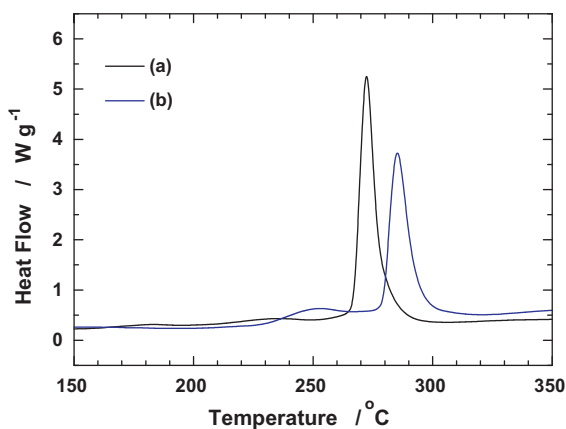


Fig. 9. Differential scanning calorimetry (DSC) traces of (a) pristine $\text{Li}_{1.1}\text{Al}_{0.05}\text{Mn}_{1.85}\text{O}_4$ and (b) AlF_3 -coated $\text{Li}_{1.1}\text{Al}_{0.05}\text{Mn}_{1.85}\text{O}_4$ at a charged state to 4.3 V.

region. The plots for the electrodes present two semicircles, one in the high-to-medium frequency region and the other in the low frequency region. The high-to-medium frequency semicircle was attributed to the resistance of the surface film (R_{sf}) covered electrode particles, and the low-frequency was attributed to the charge transfer resistance (R_{ct}). Details are described in our previous report [28,29]. The R_{sf} value was larger for the AlF_3 -coated material in the high frequency region (see inset of Fig. 8b), as the insulating AlF_3 covers the spinel active materials. The R_{sf} value became gradually larger with cycling, likely due to the resistive component like LiF on the electrode surface. Less precipitation of LiF for the AlF_3 -coated $\text{Li}_{1.1}\text{Al}_{0.05}\text{Mn}_{1.85}\text{O}_4$ produced a smaller R_{sf} value relative to the pristine spinel throughout cycling. The charge-transfer resistance (R_{ct}) of the pristine $\text{Li}_{1.1}\text{Al}_{0.05}\text{Mn}_{1.85}\text{O}_4$ was greatly increased during the cycle. Meanwhile, the R_{ct} value of the AlF_3 -coated $\text{Li}_{1.1}\text{Al}_{0.05}\text{Mn}_{1.85}\text{O}_4$ was relatively reduced. The R_{ct} value of the pristine $\text{Li}_{1.1}\text{Al}_{0.05}\text{Mn}_{1.85}\text{O}_4$ electrode at the first cycle was $21.4\ \Omega$ and significantly increased to $51\ \Omega$ after 100 cycles. However, the charge transfer resistance value of the AlF_3 -coated $\text{Li}_{1.1}\text{Al}_{0.05}\text{Mn}_{1.85}\text{O}_4$ electrode varied slightly from $5.4\ \Omega$ at the first cycle to $30.1\ \Omega$ after 100 cycles. Less deposition of LiF on the electrode surface and less dissolution of Mn due to the AlF_3 coating affected the smaller increase in impedance upon cycling. As a result, the interface between the electrode and electrolyte was significantly stabilized with the help of the AlF_3 coating layer on the spinel particles.

The thermal stability of the pristine and AlF_3 -coated $\text{Li}_{1.1}\text{Al}_{0.05}\text{Mn}_{1.85}\text{O}_4$ electrode is shown in Fig. 9. Each of these cells was charged to 4.3 V to test with DSC. The AlF_3 -coated $\text{Li}_{1.1}\text{Al}_{0.05}\text{Mn}_{1.85}\text{O}_4$ showed a major exothermic peak at $285\ ^\circ\text{C}$, while the pristine $\text{Li}_{1.1}\text{Al}_{0.05}\text{Mn}_{1.85}\text{O}_4$ showed a major exothermic peak at $272\ ^\circ\text{C}$. Additionally, the total heat generation of AlF_3 -coated $\text{Li}_{1.1}\text{Al}_{0.05}\text{Mn}_{1.85}\text{O}_4$ was reduced, as compared to the pristine $\text{Li}_{1.1}\text{Al}_{0.05}\text{Mn}_{1.85}\text{O}_4$. The pristine $\text{Li}_{1.1}\text{Al}_{0.05}\text{Mn}_{1.85}\text{O}_4$ and AlF_3 -coated $\text{Li}_{1.1}\text{Al}_{0.05}\text{Mn}_{1.85}\text{O}_4$ produced $439\ \text{J g}^{-1}$ and $315\ \text{J g}^{-1}$, respectively. This result is similar to other AlF_3 -coated layer compounds [21–24,26]. With the aid of the AlF_3 coating layer, the thermal property of the fully delithiated AlF_3 -coated $\text{Li}_{1-\delta}\text{Al}_{0.05}\text{Mn}_{1.85}\text{O}_4$ was also improved.

4. Conclusions

AlF_3 was coated on the spinel $\text{Li}_{1.1}\text{Al}_{0.05}\text{Mn}_{1.85}\text{O}_4$, and its effects on electrochemical performance were investigated. TEM analysis demonstrated a well-dispersed AlF_3 -coating

with a thickness of approximately 10–15 nm. The AlF_3 -coated $\text{Li}_{1.1}\text{Al}_{0.05}\text{Mn}_{1.85}\text{O}_4$ improved cycling performance, rate capability, and thermal stability. The capacity retention of the AlF_3 -coated $\text{Li}_{1.1}\text{Al}_{0.05}\text{Mn}_{1.85}\text{O}_4$ after 90 cycles was 96.2%, while that of the pristine $\text{Li}_{1.1}\text{Al}_{0.05}\text{Mn}_{1.85}\text{O}_4$ was 85.3%, because the presence of the AlF_3 coating layer suppressed decomposition of LiPF_6 salt, as confirmed by ToF-SIMS. The decreased HF during cycling resulted in a significant decrease in manganese dissolution from the spinel $\text{Li}_{1.1}\text{Al}_{0.05}\text{Mn}_{1.85}\text{O}_4$ material. The protection of the active material by AlF_3 coating was substantially effective for improving the capacity, capacity retention, rate capability, and thermal stabilities of the spinel cathode.

Acknowledgements

This research was supported by a grant from the Energy Technology R&D Programs of the Ministry of Knowledge Economy (MKE), of the Korean Government (No. 2008-11-0055). This work was also supported by the Korea Science and Engineering Foundation (KOSEF) grant, funded by the (MEST) of the Korean Government (No. 2009-0092780).

References

- [1] J.M. Tarascon, D. Guyomard, *J. Electrochem. Soc.* 138 (1991) 2864–2868.
- [2] T. Ohzuku, M. Kitagawa, T. Hirai, *J. Electrochem. Soc.* 137 (1990) 769–775.
- [3] J.M. Tarascon, D. Guyomard, *Electrochim. Acta* 38 (1993) 1221–1231.
- [4] M.M. Thackeray, *Prog. Solid State Chem.* 25 (1997) 1–71.
- [5] D.-H. Jang, Y.-J. Shin, S.-M. Oh, *J. Electrochem. Soc.* 143 (1996) 2204–2211.
- [6] S. Komaba, N. Kumagai, T. Sasaki, Y. Miki, *Electrochemistry* 69 (2001) 784–787.
- [7] S.-T. Myung, S. Komaba, N. Kumagai, *J. Electrochem. Soc.* 148 (2001) A482–A489.
- [8] B. Banov, Y. Todorov, A. Trifonova, A. Momchilov, V. Manev, *J. Power Sources* 68 (1997) 578–581.
- [9] K. Amine, H. Tukamoto, H. Yasuda, Y. Fujita, *J. Electrochem. Soc.* 143 (1996) 1607–1613.
- [10] K. Amine, H. Tukamoto, H. Yasuda, Y. Fujita, *J. Power Sources* 68 (1997) 604–608.
- [11] C. Sigala, A. Verbaere, J.L. Mansot, D. Guyomard, Y. Piffard, M. Tournoux, *J. Solid State Chem.* 132 (1997) 372–381.
- [12] L. Hernan, J. Morales, L. Sanchez, J. Santos, *Solid State Ionics* 118 (1999) 179–185.
- [13] J.S. Gnanaraj, V.G. Pol, A. Gedanken, D. Aurbach, *Electrochem. Commun.* 5 (2003) 940–945.
- [14] J.-M. Han, S.-T. Myung, Y.-K. Sun, *J. Electrochem. Soc.* 153 (2006) A1290–A1295.
- [15] Y.-K. Sun, K.-J. Hong, J. Prakash, *J. Electrochem. Soc.* 150 (2003) A970–A972.
- [16] M.M. Thackeray, C.S. Johnson, J.-S. Kim, K.C. Lauze, J.T. Vaughey, N. Dietz, D. Abraham, S.A. Thackeray, W. Zeltner, M.A. Anderson, *Electrochem. Commun.* 5 (2003) 752–758.
- [17] J.-S. Kim, C.S. Johnson, J.T. Vaughey, S.A. Hackney, K.A. Walz, W.A. Zeltner, M.A. Anderson, M.M. Thackeray, *J. Electrochem. Soc.* 151 (2004) A1755–A1761.
- [18] K.-S. Lee, S.-T. Myung, K. Amine, H. Yashiro, Y.-K. Sun, *J. Mater. Chem.* 19 (2009) 1995–2005.
- [19] Y.-K. Sun, J.-M. Han, S.-T. Myung, S.-W. Lee, K. Amine, *Electrochem. Commun.* 8 (2006) 821–826.
- [20] Y.-K. Sun, S.-W. Cho, S.-W. Lee, C.S. Yoon, K. Amine, *J. Electrochem. Soc.* 154 (2007) A168–A172.
- [21] S.-U. Woo, C.S. Yoon, K. Amine, I. Belharouak, Y.-K. Sun, *J. Electrochem. Soc.* 154 (2007) A1005–A1009.
- [22] Y.-K. Sun, S.-W. Cho, S.-T. Myung, K. Amine, *J. Prakash, Electrochim. Acta* 53 (2007) 1013–1019.
- [23] B.-C. Park, H.-B. Kim, S.-T. Myung, K. Amine, I. Belharouak, S.-M. Lee, Y.-K. Sun, *J. Power Sources* 178 (2008) 826–831.
- [24] H.-B. Kim, B.-C. Park, S.-T. Myung, K. Amine, J. Prakash, Y.-K. Sun, *J. Power Sources* 179 (2008) 347–350.
- [25] B.-C. Park, H.-B. Kim, H.J. Bang, J. Prakash, Y.-K. Sun, *Ind. Eng. Chem. Res.* 47 (2008) 3876–3882.
- [26] Y.-K. Sun, S.-T. Myung, B.-C. Park, H. Yashiro, *J. Electrochem. Soc.* 155 (2008) A705–A710.
- [27] K.-S. Lee, S.-T. Myung, H.J. Bang, S. Chung, Y.-K. Sun, *Electrochim. Acta* 52 (2007) 5201–5206.
- [28] Y.-J. Kang, J.-H. Kim, S.-W. Lee, Y.-K. Sun, *Electrochim. Acta* 50 (2005) 4784–4791.
- [29] Y.-K. Sun, S.-W. Cho, S.-T. Myung, K. Amine, J. Prakash, *Electrochim. Acta* 53 (2007) 1013–1019.